Published in Micro & Nano Letters
Received on 6th January 2009
Revised on 9th March 2009
doi: 10.1049/mnl.2009.0001

ISSN 1750-0443

Field emission dependence on the tilted angle of palladium nanogaps for surface conduction electron-emitter displays

Y. Li H.-W. Cheng

Department of Communication Engineering, National Chiao Tung University, 1001 Ta-Hsueh Road, Hsinchu 300, Taiwan, Republic of China
E-mail: ymli@faculty.nctu.edu.tw

Abstract: The emission efficiency of novel surface conduction electron-emitters corresponding to tilted angles (θ) of a nanogap-typed driving cathode is optimised. Among the parameters of the emitter profile, the apex angle is the most significant because the smaller angles induce a higher electric field. The higher electric field then attracts more particles into vacuum and then increases the emission current. However, the structure of the driving cathode limits the electron trajectory while the angle decreases, and it reflects that the portion of collected current by the anode decreases and results in a drop in emission efficiency. The electric field with larger tilted angles will be weakened, but most of the emitted electrons could be collected by the anode, which increases emission efficiency. This shows there is highest emission efficiency (about 37%) under an optimum angle (θ) of 60° owing to a trade-off between emission efficiency and emitter apex.

1 Introduction

A surface conduction electron-emitter display (SED) features lower material costs than a liquid crystal display (LCD); hence the manufacturing costs can be reduced. Cathodes with nanometre separation have diverse applications, such as molecular electronics [1] and vacuum microelectronics [2]. One of the emerging technologies of nanogaps is the surface conduction electron emitter (SCE) for applications of flat panel displays (FPDs), which has attracted much attention [3–9]. An SED is an advanced type of FPD based upon SCEs. The critical process step to fabricate SCEs is to create a nano figure on a line cathode for electron emission. SEDs have a high-quality image, high resolution, quick response time and low power consumption [4], but the nanogap fabrication process is complicated and expensive. The field emission (FE) efficiency and current density of these cathodes further depend on both their geometry and fabrication materials. For SCEs, the emission is obtained with a high electric field by a driving voltage that causes electrons to tunnel over a potential barrier out of the emitter to the driving cathode and anode. The emitter's geometry increases emission by enhancing the electric field and reducing the barrier over which the electrons must tunnel. A novel SCE device fabricated by hydrogen embrittlement (HE) has recently been proposed by us for its high FE property [5–8]. However, FE efficiency strongly depends on the emitter's geometry, in particular the tilted angles.

In this work, the effect of the tilted angle of the driving cathode on FE performance is theoretically examined by solving a set of three-dimensional (3D) Maxwell's equations and the Lorentz equation with the finite-difference time-domain particle-in-cell (FDTD-PIC) method [5–8]. In the FE process, electron emission is modelled by the Fowler–Nordheim (F–N) equation. As the tilted angle (θ) of Fig. 1 decreases, the emitter apex gathers a high electric field, which introduces a high emission current. But the geometry also limits particle trajectory and reduces the collected current on the anode.

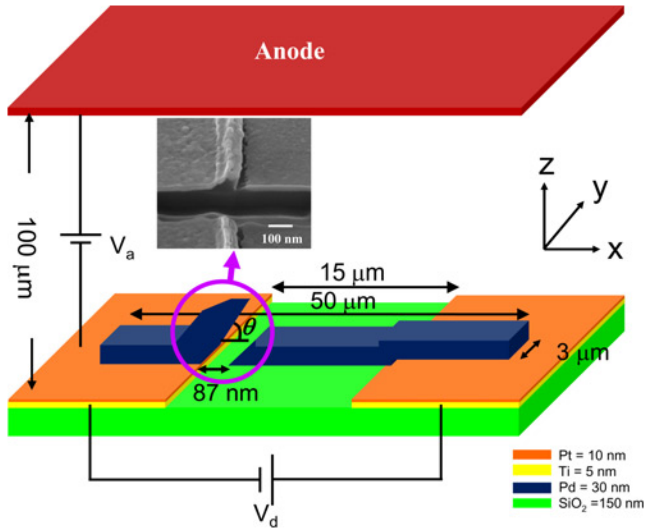

Figure 1 *The whole configuration of the SCE device fabricated by palladium hydrogenation nanogap (novel SCE), where the angle is the variable to be explored for the emission efficiency. The right corner summarises the thickness for each material. The inset is an SEM image of the fabricated sample [7]. We notice that the angle of the right-bottom electrode is equal to 30°, which was extracted from the fabricated sample*

The optimum angle is thus examined for the high emission efficiency of the novel SCE device.

This paper is organised as follows. We state the structure of the SED and simulation technique in Section 2. Results and discussion on the emission properties are shown in Section 3. Finally, we conclude from the results that there is an optimum angle for the best emission efficiency and suggest future work.

2 Structure and simulation

The configuration of novel SCE devices fabricated by hydrogen absorption is shown in Fig. 1, where an adequate value of 87 nm gap was obtained experimentally for the novel structure simulation, and is superior to the conventional one fabricated by a focused ion beam (FIB). The driving voltage of the structure is 40 V and the voltage between the cathode and anode is 1960 V. Both details of fabrication have recently been reported and could be found in our previous work [5–8].

The FE property of the explored SCE device is solved using the FDTD-PIC simulation technique [5–8]. We first formulate a calibrated simulation model with the experimental data by using the simulation program that has been developed to calculate the emission efficiency of different SCEs [5–8]. Electromagnetic particle-in-cell codes are performed in the numerical simulation. Starting from a specified initial state, we simulate electrostatic fields as its evolution in time. We then perform a time integration of Faraday's law, Ampere's law and the relativistic Lorentz equation [10, 11]

$$\begin{cases} \dfrac{\partial \boldsymbol{B}}{\partial t} = -\nabla \times \boldsymbol{E} \\ \dfrac{\partial \boldsymbol{E}}{\partial t} = -\dfrac{\boldsymbol{J}}{\varepsilon} + \dfrac{1}{\mu\varepsilon}\nabla \times \boldsymbol{B} \\ \boldsymbol{F} = q(\boldsymbol{E} + \boldsymbol{v} \times \boldsymbol{B}) \\ \dfrac{\partial \boldsymbol{x}}{\partial t} = \boldsymbol{v} \end{cases} \quad (1)$$

subject to constraints provided by Gauss's law and the rule of divergence of $\boldsymbol{B}$

$$\nabla \cdot \boldsymbol{E} = \frac{\rho}{\varepsilon} \quad \text{and} \quad \nabla \cdot \boldsymbol{B} = 0 \quad (2)$$

We notice that $\boldsymbol{E}$ and $\boldsymbol{B}$ are the electric and magnetic fields, $\boldsymbol{x}$ is the position of the charge particle, and $\boldsymbol{J}$ and ρ are the current density and charge density resulting from charge particles. The full set of time-dependent 3D Maxwell's equations is simultaneously solved to obtain electromagnetic fields. Similarly, the Lorentz force equation is solved to obtain relativistic particle trajectories. In addition, the electromagnetic fields are advanced in time at each time step. The electrons are moved according to the Lorentz equation using the fields advanced in each time step. The weighted charge density and current density at the grids are subsequently calculated. The obtained charge density and current density are successively used as sources in Maxwell's equations for advancing the electromagnetic fields. These steps are repeated for each time step until the specified number of time steps is reached. We notice that the space-charge effects are automatically included in the simulation procedure. The FDTD-PIC method [12–14] forms a self-consistent solution of the electromagnetic fields and electrons.

In the EF process, electron emission is modelled by the F–N equation [15]

$$J = \frac{AE^2}{\varphi t^2} \exp\left(\frac{-Bv(y)\varphi^{3/2}}{E}\right) \quad (3)$$

where $A = 1.541 \times 10^{-6}\,\text{A eV/V}^2$ and B is a fitting parameter in our simulation depending on the applied voltage [9] and the width of the nanogap; E is the normal component of the electric field at the emitter surface, φ is the work function of the emission material, t^2 is approximately equal to 1.1 and $v(y) = 0.95 - y^2$ with $y = 3.79 \times 10^{-5} \times E^{1/2}/\varphi$ in SI units. The emission current density is determined by (3) according to the local electric field, the work function of emitter material and geometric factors. We notice that, in the entire simulation, all the dimensions of physical quantities are the same with the experimental settings, where the model parameters and the solution method have been calibrated for best accuracy [5–8].

doi: 10.1049/mnl.2009.0001

3 Results and discussion

According to our previous studies [5–8], the electric field around the tip of a novel SCE fabricated by HE is larger and exhibits higher focus ability than that of a conventional SCE fabricated by a FIB. Therefore we further investigate the impact of a tilted angle for the novel SCE by varying the fabrication feasible range of a tilted angle. First, the physical settings of an SCE are fixed except for the tilted angle. We then focus on examining the tilted angle effect on the FE efficiency of the novel SCE. The inset of Fig. 1 shows the configuration of the novel SCE device with the specific angle of the driving cathode [5–8]. The period of time was set as 0.017 ps, at angles of 60, 50, 20, 15 and 10°, to analyse how tilted angles affect the emission efficiency. For a clear view of analysis, we pick three conditions to discuss the simulated results, which are shown in Figs. 2–4. In the beginning, electrons are emitted from the palladium (Pd) cathode [16]; when the anode voltage is increased, the emitted electrons are attracted upward. When the anode voltage continuously keeps increasing, electrons keep moving upward. Finally, about 27% of the total emitted electrons are collected by the top anode. Most of the electrons (73% of the total emitted electrons) are absorbed by boundary or materials. During the simulation process we know that the electron trajectories are affected by the electric field. By analysing the electric field, the motion of emitted electrons is described. Then the optimal geometry settings of the SCE are found. Figs. 2*a*, 3*a* and 4*a* represent the electric field and Figs. 2*b*, 3*b* and 4*b* show the electron trajectories under different angles of the emitter apex; they are 80, 60 and 10°, respectively. In these figures the electric field around the tip increases as the angle decreases owing to the formulation of an acute angle. Hence more particles are attracted, tunnel into the vacuum and make the emission current increase. The angles of the emitter apex affect the magnitude of emission current directly. Fig. 2*a* shows that the larger tilted angle induces fewer emitted electrons from the cathode because of a weak electric field. The wider distribution of the electric field benefits the electrons moving upward, as shown in Fig. 2*b*. However, the collected current on the anode is smaller because of the limitation of emitted electrons. As the angle decreases,

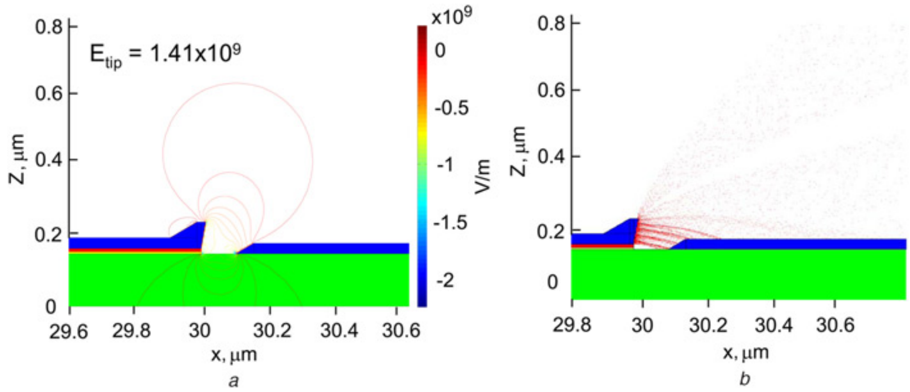

Figure 2 *Electric field distribution and electron trajectories near the gap for the device with $\theta = 80^\circ$*

a Electric field distribution near the gap for the device with $\theta = 80^\circ$
b Electron trajectories near the gap for the device with $\theta = 80^\circ$

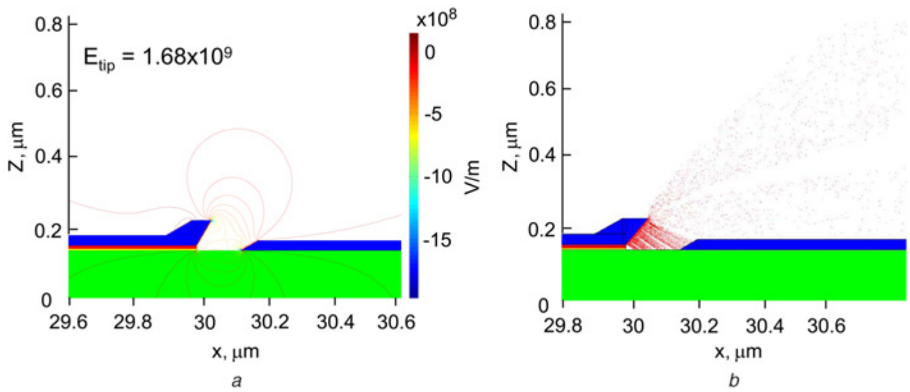

Figure 3 *Electric field distribution and electron trajectories near the gap for the device with $\theta = 60^\circ$*

a Electric field distribution near the gap for the device with $\theta = 60^\circ$
b Electron trajectories near the gap for the device with $\theta = 60^\circ$

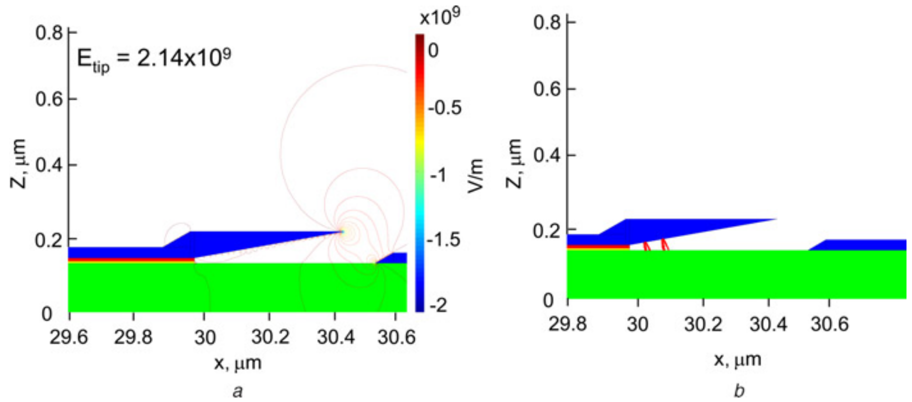

Figure 4 *Electric field distribution and electron trajectories near the gap for the device with $\theta = 10^\circ$*

a Electric field distribution near the gap for the device with $\theta = 10^\circ$
b Electron trajectories near the gap for the device with $\theta = 10^\circ$

the emitted electrons are increased because of the increased electric field. The distribution of the electric field becomes smaller owing to the lower position of the tip, as shown in Fig. 3*a*. With larger electric field around the tip, a few emitted electrons are attracted by the cathodes, as shown in Fig. 3*b*. Fewer parts of emitted electrons moving downward do not reduce the collected current, because most electrons attracted from the emitter owing to a larger electric field move upward to the anode and increase the magnitude of collected current. With a decreasing tilted angle, the electric field becomess stronger, but the collected current may reduce because of a weak electric field. The electric field is increased rapidly because of the sharp tip of the emitter, as shown in Fig. 4*a*. But the weak electric field on the sidewall of the cathode and the increasing area of cathodes, because of the fixed gap width, reduce the magnitude of collected current by the anode directly. However, Fig. 4*b* shows that most of the emitted electrons are blocked by the geometry. Figs. 5*a* and *b* summarise the magnitude of collected and emitted currents under different tilted angles of an SCE, where both peak values occur in an SCE with about a 20° tilted angle. During the simulation, the potential drop between two cathodes reduces, and this results in the time delay when particles are attracted. To evaluate FE efficiency, the ratio of emission current and collected current by the anode plate is calculated by

$$\text{emission efficiency } (\eta) = \frac{\text{collected current by anode}}{\text{emitted current by cathode}} \times 100\% \tag{4}$$

Based on such an expression, the simulated result shows that the optimal FE efficiency is determined under an angle of 60°, as shown in Fig. 6. According to the previous results, most emitted currents with larger electric fields are collected by the anode for a 20° tilted angle. We notice that a slightly increasing electric field induces a large emitted current, as shown in Fig. 5*a*. Therefore FE efficiency is highest with an appropriate tilted angle. The optimal value is determined by the electric field around the emitter apex and the distance between the two cathodes. As the angle decreases, the emitter apex extends outward and introduces a significant electric field around the tip, but the increasing area of the cathodes weakens the attraction for

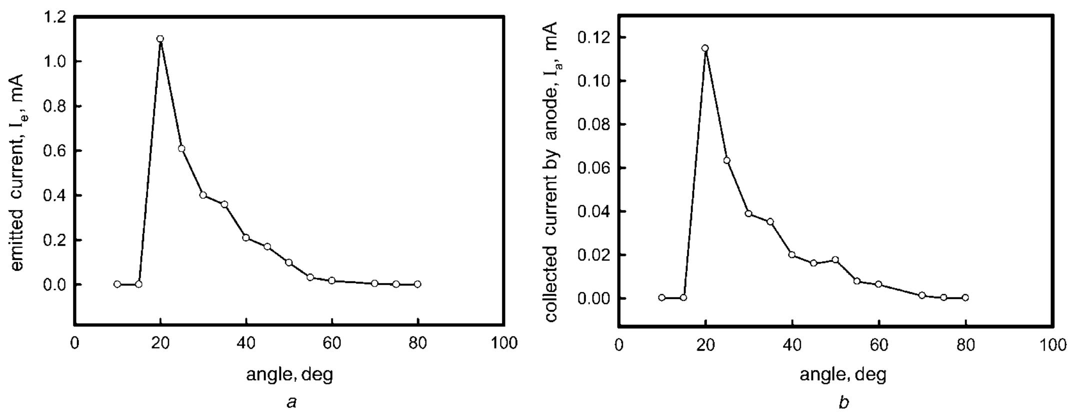

Figure 5 *Emitted current and collected current by the top anode plate against tilted angles*

a Emitted current against tilted angles
b Corresponding collected current by the top anode plate against tilted angles

doi: 10.1049/mnl.2009.0001

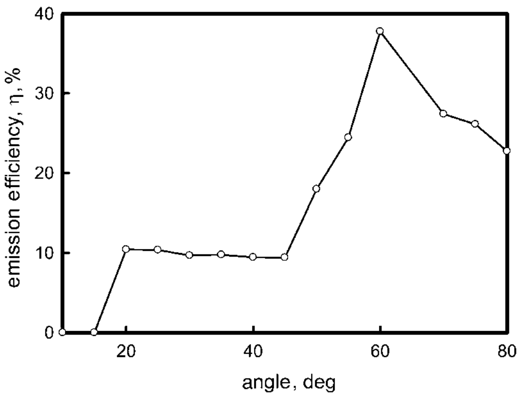

Figure 6 *Dependence of FE efficiency on different tilted angles*

particles and blocks the emitted electrons moving upward on the side wall of the emitted cathode. This trade-off for the attraction makes the optimal angle exist. The corresponding efficiency is 37% under the optimal tilted angle.

4 Conclusions

We have investigated the effect of a tilted angle of a cathode on FE property of a novel SCE. The new structure has higher focus capability than the conventional one with the vertical angle owing to the high electric field around the emitter apex. The FE efficiency of a novel SCE strongly depends on the tilted angle of the cathode; the small angle induces a strong local field and attracts emitted electrons from the cathode. Nevertheless, FE efficiency is suppressed because most of the emitted electrons are impeded by the structure with a small angle. For the case of a large angle, more emitted electrons could be found, but the emission efficiency is rather limited by a very weak electric field. Our study has suggested that a tilted angle of 60° may possess optimal FE efficiency for the novel SCE with a fixed separation width of the nanogap at 87 nm. We are currently investigating the FE property of nanogaps with different geometry configuration, cathode material and morphology.

5 Acknowledgments

This work was supported by Taiwan National Science Council (NSC) under NSC-97-2221-E-009-154-MY2 and Contract NSC-96-2221-E-009-210, and by the Chunghwa Picture Tubes, Ltd., Taiwan under a 2007–2008 grant.

6 References

[1] REED M.A., ZHOU C., MULLER C.J., BURGIN T.P., TOUR J.M.: 'Conductance of a molecular junction', *Science*, 1997, **278**, pp. 252–254

[2] LEE H.I., PARK S.S., PARK D.I., HAM S.H., LEE J.H.: 'Nanometer-scaled gap control for low voltage and high current operation of field emission array', *J. Vac. Sci. Technol. B*, 1998, **16**, pp. 762–764

[3] SAKAI K., NOMURA I., YAMAGUCHI E., *ET AL.*: 'Flat-panel displays based on surface-conduction electron-emitters', *Proc. Euro. Display*, 1996, pp. 569–572

[4] YAMAGUCHI E., SAKAI K., NOMURA I., *ET AL.*: 'A 10-in. surface-conduction electron-emitter display', *J. Soc. Inf. Disp.*, 1997, **5**, pp. 345–348

[5] LI Y., CHAO H.-Y., LO H.-Y.: 'High field emission efficiency surface conduction electron emitters', *J. Comput. Electron.*, 2008, **7**, pp. 440–444

[6] LI Y., LO H.Y.: 'Surface conduction electron emission in palladium hydrogenation nanogaps', *J. Phys. D. Appl. Phys.*, 2008, **41**, p. 085301

[7] LO H.Y., LI Y., CHAO H.Y., TSAI C.H., PAN F.M.: 'Field-emission properties of novel palladium nanogaps for surface conduction electron-emitters', *Nanotechnology*, 2007, **18**, p. 475708

[8] LO H.Y., LI Y., TSAI C.H., CHAO H.Y., PAN F.M.: 'Effect of process variation on field emission characteristics in surface conduction electron-emitters', *IEEE Trans. Nanotech.*, 2008, **7**, pp. 434–439

[9] LO H.Y., LI Y., TSAI C.H., PAN F.M.: 'Analysis of field emission of fabricated nanogap in Pd strips for conduction electron-emitter displays', *Jpn. J. Appl. Phys.*, 2008, **47**, p. 2972

[10] GOTH Y., OHTAKE T., FUJITA N., INOUE K., TSUJI H., ISHIKAWA J.: 'Fabrication of lateral-type thin-film edge field emitters by focus ion beam technique', *J. Vac. Sci. Technol. B*, 1995, **13**, pp. 465–468

[11] STERN T.E., GOSLING B.S., FOWLER R.H.: 'Further studies in the emission of electrons from cold metals', *Roy. Soc. Proc. A*, 1929, **124**, pp. 699–723

[12] VERBONCOEUR J.P., LANGDON A.B., GLADD N.T.: 'An object-oriented electromagnetic PIC code', *Comput. Phys. Commun.*, 1995, **87**, pp. 199–211

[13] GOPLEN B., LUDEKING L., SMITHE D., WARREN G.: 'User-configurable MAGIC for electromagnetic PIC simulation', *Comput. Phys. Commun.*, 1995, **87**, pp. 54–86

[14] BIRDSALL C.K., LANGDON A.B.: 'Plasma physics via computer simulation' (McGraw-Hill, New York, 1985)

[15] FOWLER R.H., NORDHEIM L.W.: 'Electron emission in intense electric fields', *Proc. R. Soc. London A*, 1928, **119**, pp. 173–181

[16] MICHAELSON H.B.: 'The work function of the elements and its periodicity', *J. Appl. Phys.*, 1977, **48**, pp. 4729–4730

doi: 10.1049/mnl.2009.0001